

### 130. Solution Structures of One-Electron Reduced and Oxidized Molecules with Twisted Donor and Acceptor Moieties

by Henning Hopf, Martin Kreutzer, and Cornelia Mlynec

Institut für Organische Chemie der Universität Braunschweig, Hagenring 30, D-38106 Braunschweig

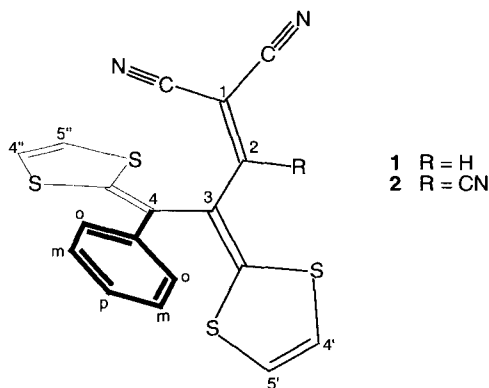
and Markus Scholz and Georg Gescheidt\*

Institut für Physikalische Chemie der Universität Basel, Klingelbergstrasse 80, CH-4056 Basel

(16.III.94)

The solution structures of the radical anion and the radical cation of the donor-acceptor molecules 3,4-di(1,3-dithiol-2-ylidene)-4-phenylbut-1-ene-1,1-dicarbonitrile (**1**) and 3,4-di(1,3-dithiol-2-ylidene)-4-phenylbut-1-ene-1,1,2-tricarbonitrile (**2**) are discussed based on cyclovoltammetric and ESR/ENDOR measurements. It is shown that the spin population of the radical anions is limited to the di- and tricyanoethene moiety and the coplanar 1,3-dithiole at C(3), whereas that of the radical cations resides mainly inside the two 1,3-dithiole rings. The energies of the long-wave bands in the electronic-absorption spectra of **1** and **2** correspond to the differences between the oxidation and reduction potentials and thus point to a charge-transfer character of these transitions.

**Introduction.** – Organic materials indicating charge-transfer interactions are playing an important role in the development of conductors [1] or opto-electronic devices [2]. Whereas one class of such compounds involves charge-transfer complexes [3] of donors (*e.g.*, tetrathiafulvalene, TTF) and acceptors (*e.g.*, tetracyanoquinodimethane, TCNQ), recently synthesized molecules comprise both functionalities in a geometry allowing spiroconjugation [4]. Compounds **1** (3,4-di(1,3-dithiol-2-ylidene)-4-phenylbut-1-ene-1,1-dicarbonitrile) and **2** (3,4-di(1,3-dithiol-2-ylidene)-4-phenylbut-1-ene-1,1,2-tricarbonitrile) [5] are composed of efficient acceptor and donor fragments. The electron-accepting part of these molecules is the di- or tricyanoethene whereas the 1,2-di(1,3-dithiol-2-ylidene)ethane moiety serves as the electron donor.



The crystal structure of **2** indicates that the tricyanoethenyl group and the 1,3-dithiole at C(3) are coplanar but almost orthogonal to the second part of the molecule, *i.e.*, the Ph substituent and the second 1,3-dithiole [5]. A very similar geometry should also hold for **1**.

Here, we investigate the influence of the restricted geometry, *i.e.*, the close proximity but twisted arrangement of the donor and acceptor moieties within the molecule, on the electron-transfer behavior of **1** and **2**. Moreover, we shed some light onto the solution structure of the one-electron reduced and oxidized stages of **1** and **2** on the hyperfine time-scale provided by ESR spectroscopy.

Compound (<sup>2</sup>H<sub>5</sub>)-**1** in which the H-atoms of the Ph ring are replaced by <sup>2</sup>H is also included [5]<sup>1)</sup>. The analysis of the ESR spectra of ((<sup>2</sup>H<sub>5</sub>)-**1**)<sup>•-</sup>/((<sup>2</sup>H<sub>5</sub>)-**1**)<sup>•+</sup> in comparison to **1**<sup>•-</sup>/**1**<sup>•+</sup> and **2**<sup>•-</sup>/**2**<sup>•+</sup> allows to substantiate the assignment of the proton-hyperfine coupling constants, and thus helps to gain a conclusive information about electron delocalization.

**Experimental.** – Cyclovoltammograms were recorded on a *Metrohm* instrument (Polarecord E 506, VA scanner E 612, VA stand 663); working electrode: Pt disk; counterelectrode: Pt wire; reference electrode: Ag/AgCl (3M KCl); solvent: MeCN; supporting electrolyte: Bu<sub>4</sub>N<sup>+</sup>ClO<sub>4</sub><sup>-</sup> (0.1M); scan rate 300 mV · s<sup>-1</sup>.

ESR Spectra were taken on a *Varian E9* spectrometer equipped with a *Marconi Instruments 2440* microwave counter and a *Bruker ER 035 M* NMR gaussmeter for the determination of the *g* factors. ENDOR and TRIPLE measurements were performed on a *Bruker ESP 300* spectrometer system.

**Results.** – *Electrochemistry.* Fig. 1 shows the cyclic voltammograms of **1** and **2**. Both compounds are able to take up two electrons. Whereas both reduction waves indicate reversible redox processes for the tricyano derivative **2** ( $E_{1/2}^{-1} = -0.55$  V and  $E_{1/2}^{-2} = -1.21$  V vs. Ag/AgCl) only the first reduction step is reversible for the dicyano derivative **1**. The potentials of **1** are shifted to more negative values ( $E_{1/2}^{-1} = -1.12$  V and  $E_p^{-2} = -1.88$  V vs. Ag/AgCl).

Reversible oxidation waves are detected for **1** and **2**; the potentials,  $E_{1/2}^{+1}$  are rather similar (0.76 and 0.85 V vs. Ag/AgCl, respectively).

*ESR Spectroscopy. Radical Anions.* Reduction of **1** with K metal in 1,2-dimethoxyethane (DME) led to the ESR spectrum indicated in Fig. 2. The signal is split into two sets of lines due to a hyperfine-coupling constant of one proton ( $a_H = -0.776$  mT). The set at high field possesses narrower lines than that at low field, but the linewidths inside those two sets follow the opposite way. The coupling constants and the *g* value are given in Table 1. The ESR spectra of ((<sup>2</sup>H<sub>5</sub>)-**1**)<sup>•-</sup> and **1**<sup>•-</sup> are very much alike and the ENDOR technique confirms that the ESR parameters for ((<sup>2</sup>H<sub>5</sub>)-**1**)<sup>•-</sup> and **1**<sup>•-</sup> are identical (Table 1).

As a consequence of the replacement of the proton in the electron-accepting moiety of the molecule by the CN group on going from **1** to **2**, the  $a_H$  of  $-0.776$  mT is replaced by a <sup>14</sup>N coupling constant of *ca.* 0.15 mT; thus the ESR signal of **2**<sup>•-</sup> consists of one signal group. Again, this ESR signal displays a marked anisotropy (broader lines at high field) which diminishes at higher temperatures. Three  $a_H$  can be detected in the ENDOR spectrum ( $-0.048$ ,  $-0.025$ , and  $+0.011$  mT). The simulation of the ESR spectrum establishes that all  $a_H$  are due to one proton, and that the <sup>14</sup>N-coupling constants,  $a_N$ , are 0.1 (2 N) and 0.15 (1 N) mT (Table 1).

<sup>1)</sup> Preparation of **1**, (<sup>2</sup>H<sub>5</sub>)-**1**, and **2** will be published elsewhere [5b].

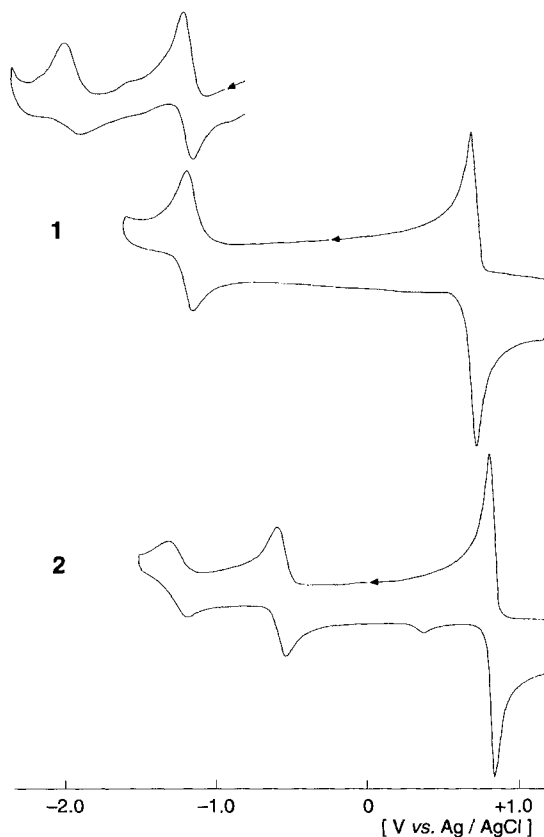


Fig. 1. Cyclovoltammograms of **1** and **2**. The insert above the cyclovoltammogram of **1** indicates the irreversible reduction to  $1^{2-}$ .

Table 1. Experimental and Calculated Proton- and Nitrogen-Hyperfine-Coupling Constants [mT] as well as *g* Factors of the Radical Anions of **1**, ( $^2\text{H}_5$ )-**1**, and **2**

Assignment	H–C(2)	H–C(4')	H–C(5')	H–C(4'' or 5'')	$H_o$	$H_m$	$H_p$	CN–C(1)	CN–C(1)	CN–C(2)	<i>g</i> Factor
Exper.											
<b>1</b> $^{\cdot-}$	–0.776	–0.076	–0.027	+0.014	–	–	–	0.075	0.061	–	2.0039
(( $^2\text{H}_5$ )- <b>1</b> ) $^{\cdot-}$	–0.776	–0.076	–0.027	+0.014	–	–	–	0.075	0.061	–	2.0039
<b>2</b> $^{\cdot-}$		–0.048	–0.025	+0.011	–	–	–	0.10	0.10	0.15	2.0040
Calc. (HMO)*											
<b>1</b> $^{\cdot-}$	–0.76	–0.03	–0.03	0.0	0.0	0.0	0.0	0.09	0.09	–	
<b>2</b> $^{\cdot-}$		–0.04	–0.04	0.0	0.0	0.0	0.0	0.09	0.09	0.18	

\* Parameters for heteroatoms:  $h_S = 1.0$ ,  $k_{CS} = 0.7$ ,  $h_N = 1.0$ ,  $k_{CN} = 2.0$ ,  $k_{C(3)C(4)} = 0.2$ . Coupling constants calculated using first-order spin populations,  $Q_H = -2.5$  mT,  $Q_N = 1.9$  mT.

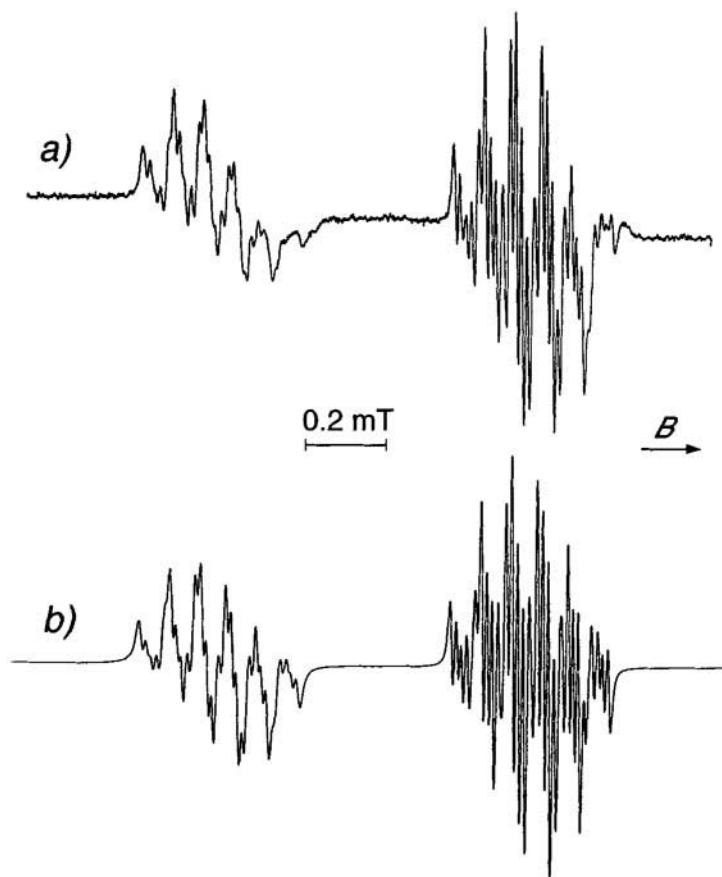


Fig. 2. ESR Spectrum of  $1^{\bullet+}$  (a, solvent: DME, counterion:  $K^+$ , temp.: 223 K) and its simulation (b)

**Radical Cations.** The radical cations of **1**, ( $^2H_5$ )-**1**, and **2** were accessible by oxidation with tris(4-bromophenyl)ammoniumyl hexachloroantimonate [6] in  $CH_2Cl_2$  as the solvent. The ESR spectra of  $1^{\bullet+}$  and  $2^{\bullet+}$  are unresolved having a width of *ca.* 1 mT; that of  $((^2H_5)-1)^{\bullet+}$  is split into three lines spaced by *ca.* 0.15 mT (spectral width *ca.* 0.6 mT). ENDOR spectroscopy allows the determination of the proton-coupling constants (Fig. 3). For  $1^{\bullet+}$ , the  $a_H$  of 0.178, 0.121, 0.099, 0.079, 0.053, 0.041, and 0.028 mT are determined (Table 2). The ENDOR spectrum of  $((^2H_5)-1)^{\bullet+}$  is identical except the missing signals for the  $a_H$  are replaced by deuterium-coupling constants (Fig. 3). In the case of  $2^{\bullet+}$ , the  $a_H$  are 0.180, 0.111, 0.091, 0.073, and 0.035 mT (Table 2). The ENDOR signals belonging to the latter  $a_H$  centered at 15.1 and 14.0 MHz are rather broad but cannot be resolved further; comparison with the  $a_H$  of  $1^{\bullet+}$  implies that the  $a_H$  of *ca.* 0.053, 0.041, and 0.028 mT are enveloped inside these lines. From the simulations of the ESR spectra,  $a_N$  can be estimated to be  $<0.05$  mT.

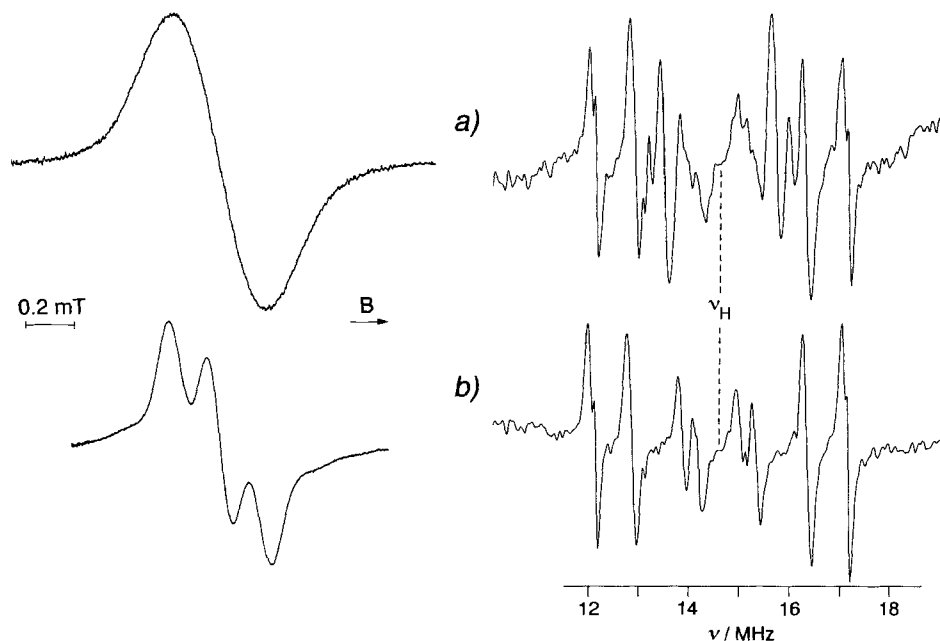


Fig. 3. ESR Spectra (left) of  $1^{\bullet\bullet}$  (a) and  $((^2\text{H}_3)\text{-}1)^{\bullet\bullet}$  (b) and the corresponding ENDOR spectra (right). Solvent:  $\text{CH}_2\text{Cl}_2$ , counterion:  $\text{SbCl}_6^-$ , temp.: 243 K.

Table 2. Experimental and Calculated Proton-Hyperfine-Coupling Constants [mT] as well as  $g$  Factors of the Radical Cations of  $1$ ,  $(^2\text{H}_3)\text{-}1$ , and  $2$

Assignment	H-C(4'') <sup>a)</sup>	H-C(5'') <sup>a)</sup>	H <sub>p</sub> <sup>b)</sup>	H <sub>o</sub> <sup>b)</sup>	H-C(4') <sup>c)</sup>	H <sub>m</sub>	H-C(5') <sup>c)</sup>	$g$ Factor
Exper.								
$1^{\bullet\bullet}$	0.178	0.121	0.099	0.079	0.053	0.041	0.028	2.0072
$((^2\text{H}_3)\text{-}1)^{\bullet\bullet}$	0.180	0.124				0.053	0.029	2.0072
$2^{\bullet\bullet}$	0.180	0.111	0.091	0.073	0.035 <sup>d)</sup>	0.035 <sup>d)</sup>	0.035 <sup>d)</sup>	2.0072
Calc. (HMO) <sup>e)</sup>								
$1^{\bullet\bullet}$ and $2^{\bullet\bullet}$	0.17	0.17	0.10	0.10	0.07	0.04	0.07	

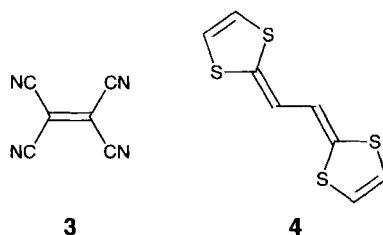
<sup>a)</sup><sup>c)</sup> Assignment based on comparison with the data in [11]; however, these  $a_{\text{H}}$  may be interchanged. <sup>b)</sup> These  $a_{\text{H}}$  may be interchanged. <sup>d)</sup> Broad ENDOR signal which presumably comprises three coupling constants of comparable size.

<sup>e)</sup> Parameters for heteroatoms:  $h_{\text{S}} = 1.0$ ,  $k_{\text{CS}} = 0.7$ ,  $h_{\text{N}} = 1.0$ ,  $k_{\text{CN}} = 2.0$ ,  $k_{\text{C(3)C(4)}} = 0.2$ ,  $k_{\text{C(2)C(3)}} = k_{\text{C(4)Ph}} = 0.7$ . Coupling constants calculated based on spin populations using the McLachlan procedure,  $Q_{\text{H}} = -2.5$  mT,  $Q_{\text{N}} = 1.9$  mT.

**Discussion. – Radical Anions.** The first reduction potentials of  $-1.12$  and  $-0.55$  V vs. Ag/AgCl of **1** and **2**, respectively, represent the enhanced electron accepting capability on replacing one H-atom by a CN group. Still, **1** and **2** are worse electron acceptors than tetracyanoethene (**3**;  $E_{1/2} = -0.24$  V vs. Ag/AgCl [7]).

The results of the cyclovoltammetric measurements only represent thermodynamic and kinetic stabilities; structural features and the amount of spin delocalisation in **1** $^{\cdot-}$  and **2** $^{\cdot-}$  are provided by the ESR/ENDOR/TRIPLE spectroscopies.

The ESR spectra of **1** $^{\cdot-}$  and  $((^2\text{H}_5)\text{-1})^{\cdot-}$  indicate identical hyperfine data (Table 1). This means that no detectable spin population resides in the phenyl substituent. The assignment of the  $a_{\text{H}}$  of  $-0.776$  mT $^2$  to the single proton at C(2) is straightforward, and, thus, the  $a_{\text{H}}$  of  $-0.076$ ,  $-0.027$ , and  $+0.014$  mT must belong to the four non-equivalent H-atoms at the two 1,3-dithiols. The two negative  $a_{\text{H}}$  with the higher values are ascribed to the H-atoms at the 1,3-dithiole ring at C(3) which, according to the X-ray structure of **2**, is oriented coplanar to the dicyanoethene moiety. The remaining coupling constant of  $+0.014$  mT (1 H) consequently must be allotted to one of the protons at the second 1,3-dithiole at C(4); the other proton carries no detectable spin population. As presented in Table 1, HMO calculations predict only very roughly the spin distribution in **1** $^{\cdot-}$  and **2** $^{\cdot-}$ , presumably because the standard parameters for the S-atom do underestimate the ability of S-atoms for the delocalisation of the negative charge $^3$ ). The  $g$  factors of **1** $^{\cdot-}$ ,  $((^2\text{H}_5)\text{-1})^{\cdot-}$ , and **2** $^{\cdot-}$  are in the same range as those of related electron acceptors as tetracyanoethene [8], tetracyanoquinodimethane [9], or 2,2'-(furan-2,5-diylidimethylidene)bispropanedinitrile [10] ( $g = 2.0026, 2.0027, 2.0039$ , respectively).



**Radical Cations.** The oxidation potentials of **1** and **2** are considerably higher (Fig. 1) than those of the related donor 1,2-di(1,3-dithiol-2-ylidene)ethene (**4**;  $0.24$  V vs. Ag/AgCl [11]). Two factors should be responsible for these diminished donor properties of **1** and **2**: i) electron density is withdrawn from the  $\pi$  system of the 1,2-di(1,3-dithiol-2-ylidene)ethane fragment by the electron accepting (1,1-dicyano- or 1,1,2-tricyanoethene) moiety and/or ii) the geometry of **1** $^{+\cdot}$  and **2** $^{+\cdot}$  in solution resembles that of **2** in the solid state and thus impairs delocalisation inside the entire donor  $\pi$  system. An answer to this assumptions is given by the ESR data of **1** $^{+\cdot}$ ,  $((^2\text{H}_5)\text{-1})^{+\cdot}$ , and **2** $^{+\cdot}$ .

<sup>2</sup>) The negative sign of this coupling constant can directly be derived from the observation of the broadened low-field line which is characteristic of negative coupling constants. On the other hand, the broadened high-field lines inside these two line groups point to a positive  $^{14}\text{N}$ -coupling constant.

<sup>3</sup>) It is, in our eyes, not appropriate to change the HMO parameters as long as a perfect match between experimental and calculated coupling constants is reached. This certainly leads to an overinterpretation of the simple HMO model for the heteroatom-rich and non-planar molecules **1** and **2**.

The marked difference between the ESR spectra of radical anions  $1^{\cdot-}$  and  $2^{\cdot-}$  is missing for the radical cations  $1^{\cdot+}$  and  $2^{\cdot+}$ . The  $a_H$  detected for  $1^{\cdot+}$  and  $2^{\cdot+}$  are very similar. This mirrors that the electron-accepting di- (tri-)cyanoethene moieties have no influence on the spin distribution in  $1^{\cdot+}$  and  $2^{\cdot+}$ .

In contrast to the radical anions, the ESR/ENDOR spectra of  $1^{\cdot+}$  and  $((^2H_5)-1)^{\cdot+}$  are different: the  $a_H$  of 0.099, 0.079, and 0.041 mT are missing for  $((^2H_5)-1)^{\cdot+}$  and must, therefore, be ascribed to the *ortho* (2 H), *para* (1 H), and *meta* (2 H) protons of the Ph substituent. Consequently, the remaining  $a_H$  reflect the spin distribution inside the 1,2-di(1,3-dithiol-2-ylidene)ethane moiety. In respect to the  $a_H$  found for  $4^{\cdot+}$  [11], the  $a_H$  of 0.178 and 0.121 mT must be assigned to the two protons in the 1,3-dithiole at C(4) which carries the major part of the spin population leaving the  $a_H$  of 0.053 and 0.028 mT to the 1,3-dithiole at C(3). The  $a_H$ -ratios 0.178/0.121 and 0.053/0.028 of 1.5 and 1.8 are in very good agreement with the corresponding ratio in  $4^{\cdot+}$  ( $a_H = 0.123$  and  $0.082$  mT; ratio = 1.5, see [11]). It is noteworthy that the sum of the four  $a_H$  of  $1^{\cdot+}$  ( $((^2H_5)-1)^{\cdot+}$ ,  $2^{\cdot+}$ ) is very close to that of  $4^{\cdot+}$ , i.e., 0.38 vs. 0.41 mT, respectively, thus pointing out that spin population is indeed concentrated inside the 1,2-di(1,3-dithiol-2-ylidene)-1-phenylethane fragment of  $1^{\cdot+}$  ( $((^2H_5)-1)^{\cdot+}$ ,  $2^{\cdot+}$ ). This spin population is, however, unevenly distributed between the two 1,3-dithioles. The 1,3-dithiole at C(4) of  $1^{\cdot+}$  ( $((^2H_5)-1)^{\cdot+}$ ,  $2^{\cdot+}$ ) bears *ca.* four times the amount of spin as that at C(3).

An additional indicator for the spin distribution, particularly for radical ions possessing heavy (e.g. second row) heteroatoms carrying a high spin population, is the *g* factor. The *g* factor of radical cation  $4^{\cdot+}$  is 2.0081 [11]. For  $1^{\cdot+}$ ,  $((^2H_5)-1)^{\cdot+}$ , and  $2^{\cdot+}$  a *g* factor of 2.0072 was determined. This values are clearly distinct from the *g* factor of the free electron, 2.0023. The deviation is grounded on a high spin population at the S-atoms [12]. For related donors possessing four S-atoms, the relationship:

$$g = 2.00379 + 0.03564\rho_s$$

where  $\rho_s$  is the spin population at one S-atom, has been developed [11], and for  $4^{\cdot+}$   $\rho_s = 0.121$  was established. Based on the above formula using the observed *g*-factor shifts, the spin population inside the 1,2-di(1,3-dithiol-2-ylidene)ethane moiety of  $1^{\cdot+}$ ,  $((^2H_5)-1)^{\cdot+}$ , and  $2^{\cdot+}$  is *ca.* 80% of that of  $4^{\cdot+}$ . The remaining 20% of the spin population must be predominately delocalized inside the Ph substituent because the substitution of the H-atom in the acceptor moiety by a CN group does not alter the  $a_H$  and the *g* factor. About the same spin distribution was found for Me-substituted and Ph-annelated derivatives of **4** [11].

*Calculations and Structural Considerations.* AM1 [13] calculations of **1** starting from a geometry corresponding to that found for **2** in the solid state indicate a shallow energy surface, e.g., a considerable amount of twist around the C(3)–C(4) bond is possible without a considerable change of energy. Furthermore, the Ph group at C(4) can rotate almost freely within a range of *ca.* 20°. Without a well defined geometry of **1**, **2** and their radical ions it is impossible to gain insightful hyperfine parameters by a semiempirical SCF procedure. Fig. 4 shows the highest occupied (HOMO) and the lowest unoccupied molecular orbital (LUMO) of **1** calculated by the HMO procedure. For the HMO model, the squares of the coefficients in the singly occupied molecular orbital are proportional, in first order, to the hyperfine-coupling constants [14]. The HMO-calculated HOMO and

LUMO offer only an incomplete picture of the  $\pi$ -electron distribution in **1**, **2** and their radical anions and cations (*Tables 1* and *2*). However, the comparison between the theoretical (HMO) and the experimental  $a_H$  allows some useful qualitative structural considerations.

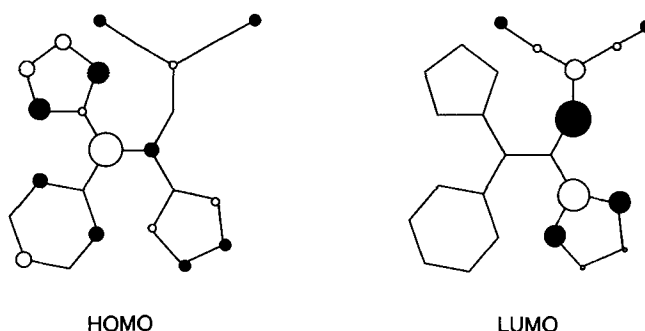


Fig. 4. HOMO and LUMO of **1** calculated by the HMO method (for parameters, see *Tables 1* and *2*)

In the LUMO of **1**, the singly occupied orbital of the radical anion, the coefficients at the 1,3-dithiole and the Ph substituent at C(4) remain almost zero irrespective of the parameters used to model the torsion around the C(3)–C(4) bond. Consequently, also the  $a_H$  predicted by the HMO model are zero; therefore, no clear evidence about a higher degree of planarity of **1** $^{\cdot-}$  and **2** $^{\cdot-}$  compared to the neutral molecules can be gained based on the calculations. Experimentally, however, spin delocalisation into the 1,3-dithiole ring at C(4) of **1** $^{\cdot-}$  and **2** $^{\cdot-}$  is established (*Table 1*); the only indication about the conformation around the C(3)–C(4) bond of **1** $^{\cdot-}$  and **2** $^{\cdot-}$  is the positive sign of the  $a_H$  of 0.014 mT which we assign to one proton at the 1,3-dithiole attached to C(4). Because of the very small MO coefficients in this 1,3-dithiole it is not probable that the positive sign is caused by a  $\pi$ - $\pi$  spin-polarisation mechanism [15]. A conceivable rationalisation for the small  $a_H$  is a through-space spin transfer (homohyperconjugation) from a  $\pi$ -orbital of the close but not directly bound atom of one cyano group. This assumption implies a geometry closer to planarity than established for neutral **2**.

The considerably higher oxidation potentials of **1** and **2** compared to **4** bear out a hindered interaction between the two 1,3-dithioles. If this situation is accounted for by  $k_{C(3)C(4)} = 0.2$  in the HMO model, the spin distribution represented by the ESR data and predicted by the model show a good agreement (*Table 2*). The two non-coplanar (almost perpendicular) 1,3-dithioles, however, still form a delocalised  $\pi$  system.

**Conclusions.** – The cyclovoltammetric and ESR/ENDOR investigations have shown that the donor-acceptor molecules **1**, ( $^2H_5$ )-**1**, and **2** resemble distinct characteristics specific of the two different redox stages.



In the radical anions the spin population is confined to the di- (tri-)cyanoethene moiety of the molecule and the coplanar 1,3-dithiole at C(3). Presumably, the geometries of  $1^{\cdot-}$ ,  $((^2\text{H}_5)\text{-}1)^{\cdot-}$ , and  $2^{\cdot-}$  are very similar to that of **2** in the solid state with a slightly more planar arrangement of the substituents at C(3) and C(4).

On the other hand, the radical cations  $1^{\cdot+}$ ,  $((^2\text{H}_5)\text{-}1)^{\cdot+}$ , and  $2^{\cdot+}$  indicate spin delocalisation across the C(3)–C(4) bond which divides these molecules into two (almost) orthogonal moieties. Despite the divergence from planarity, a considerable amount of spin (*ca.* 20%) can be found in the unfavorably arranged (in terms of  $\pi$ -conjugation) 1,3-dithiole at C(3).

The UV/VIS spectra of **1**,  $(^2\text{H}_5)\text{-}1$ , and **2** are identical [5] except the long-wave band which has to be considered as a HOMO-LUMO charge-transfer transition [16]. The bathochromic shift of this band from 462 to 525 nm on going from **1** ( $(^2\text{H}_5)\text{-}1$ ) to **2** agrees very well with the HOMO-LUMO gaps reflected by the differences between the first oxidation and reduction potentials ( $\Delta E_{1/2}$ ): the higher excitation energy for **1** is anticipated by  $\Delta E_{1/2} = 1.88$  V, whereas the longer-wave absorption of **2** is in line with  $\Delta E_{1/2} = 1.40$  V. These energy differences are particularly grounded on the less negative reduction potential of **2**.

Such charge-transfer transitions are important factors for nonlinear optical properties of molecules. Therefore, based on our results, the investigation of the electron- and charge-transfer behavior of **1** and **2** in the solid state should present further interesting insights.

We thank the Swiss National Science Foundation and the Fonds der Chemischen Industrie for financial support. G.G. thanks the Freiwillige Akademische Gesellschaft, Basel, for a Treubel Fonds scholarship.

#### REFERENCES

- [1] J. H. Perlstein, *Angew. Chem.* **1977**, 89, 534; A. F. Garito, A. J. Heeger, *Acc. Chem. Res.* **1974**, 7, 232.
- [2] D. J. Williams, *Angew. Chem.* **1984**, 96, 637; R. W. Munn, C. N. Ironside, 'Principles and Applications of Nonlinear Optical Materials', Blackie Academic & Professional, London, 1993.
- [3] A. Aumüller, E. Hädicke, S. Hünig, A. Schätzle, J.-U. v. Schütz, *Angew. Chem.* **1984**, 96, 439; A. Aumüller, P. Erk, S. Hünig, H. Meixner, J.-U. v. Schütz, H.-P. Werner, *Liebigs Ann. Chem.* **1987**, 997.
- [4] P. Maslak, A. Chopra, *J. Am. Chem. Soc.* **1993**, 115, 9331; U. Schöeberl, J. Salbeck, J. Daub, *Adv. Mater.* **1992**, 4, 41.
- [5] a) H. Hopf, M. Kreutzer, P. G. Jones, *Angew. Chem. Int. Ed.* **1991**, 30, 1127; b) H. Hopf, C. Mlynek, M. Kreutzer, *Chem. Ber.*, to be published.
- [6] F. A. Bell, A. Ledwith, D. C. Sherrington, *J. Chem. Soc. C* **1969**, 2719.
- [7] L. Meites, P. Zuman, W. J. Scott, B. H. Campbell, A. M. Kardos, T. L. Fenner, E. B. Rupp, L. Lampugani, R. Zuman, 'CRC Handbook Series in Organic Electrochemistry', CRS Press, Cleveland, 1977, Vol. I.
- [8] W. D. Phillips, J. C. Rowell, S. I. Weissman, *J. Chem. Phys.* **1960**, 33, 626.
- [9] F. Gerson, R. Heckendorn, D. O. Cowan, A. M. Kini, M. R. Maxfield, *J. Am. Chem. Soc.* **1983**, 105, 7017.
- [10] M. Scholz, G. Gescheidt, U. Schöeberl, J. Daub, *J. Chem. Soc., Perkin Trans. 2* **1992**, 2137.
- [11] A. Terahara, H. Ohya-Nishiguchi, N. Hirota, H. Awaji, T. Kawase, S. Yoneda, T. Sugimoto, Z. Yoshida, *Bull. Chem. Soc. Jpn.* **1984**, 57, 1760.
- [12] N. M. Atherton, 'Electron Spin Resonance, Theory and Applications', Wiley, New York, 1973.
- [13] M. J. S. Dewar, E. G. Zeebisch, E. F. Healy, J. J. P. Stewart, *J. Am. Chem. Soc.* **1985**, 107, 3902.
- [14] H. M. McConnell, *J. Chem. Phys.* **1956**, 24, 632.
- [15] A. D. McLachlan, *Mol. Phys.* **1960**, 3, 233.
- [16] M. Klessinger, J. Michl, 'Lichtabsorption und Photochemie organischer Moleküle', VCH, Weinheim-New York, 1989.